

# Preparation and Characterization of Hybrid Organic–Inorganic Epoxide-Based Films and Coatings Prepared by the Sol–Gel Process

Milena Špírková, Jiří Brus, Drahomíra Hlavatá, Helena Kamišová, Libor Matějka, Adam Strachota

*Institute of Macromolecular Chemistry, Academy of Sciences of the Czech Republic, Heyrovského Sq. 2, 162 06 Prague 6, Czech Republic*

Received 7 March 2003; accepted 18 September 2003

**ABSTRACT:** Hybrid organic–inorganic coatings and free-standing films were prepared and characterized. The hybrids were prepared from [3-(glycidyoxy)propyl]trimethoxysilane, diethoxy[3-(glycidyoxy)propyl]methylsilane, poly(oxypropylene)s of different molecular weights end-capped with primary amino groups (Jeffamines D230, D400, and T403), and colloidal silica particles with hydrochloric acid as a catalyst for the sol–gel process and water/propan-2-ol mixtures as solvents. The structure evolution during the network formation was followed by NMR spectroscopy and small-angle X-ray scattering; the surface morphology was tested by atomic force microscopy. The influence of the

reaction conditions (the organosilicon precursor, oligomeric amine, ratio of functional groups, and method of preparation) on the network buildup and product properties was studied and examined. The mechanical testing, based on stress–strain experiments, in combination with dynamic mechanical thermal analysis served as an effective instrument for the optimization of the reaction conditions for the preparation of products with desired properties. © 2004 Wiley Periodicals, Inc. *J Appl Polym Sci* 92: 937–950, 2004

**Key words:** films; coatings; NMR; atomic force microscopy (AFM); SAXS; mechanical properties

## INTRODUCTION

New nanocomposite materials with desired mechanical properties can be designed and manufactured if the heterogeneity on the nanometer scale can be controlled and optimized. Because the molecular-scale morphology plays an important role in achieving desirable macroscopic properties of molecular and supramolecular assemblies, the synthetic goal is to prepare multiphase microheterogeneous systems with tunable properties. Organic–inorganic (O–I) hybrid polymers with an *in situ* created inorganic phase are typical examples of promising nanocomposite materials. The modification of the organic matrix with silica–siloxane domains formed by the sol–gel process of alkoxy silanes is one of the methods of their preparation. The resulting structures formed in the sol–gel process depend on the reaction conditions and vary from monodisperse silica particles to polymer networks.<sup>1–8</sup>

The production of new materials with specialty functions requires detailed information on the structure–property relationship. Designing materials with well-adjusted properties makes possible their potential use in industrial applications with specific requirements, such as coatings for various kinds of protection<sup>9–13</sup> (scratch-, abrasion-, corrosion-, hydrolytic-, and oxygen-resistant systems).

Trialkoxysilanes of the formula  $R'-Si-(OR)_3$ , where  $R'$  is a short hydrocarbon chain bearing an organic functional group (e.g., epoxy, amino, isocyanate, methacryloyl, or vinyl) and  $R$  is an alkyl group, are widely used monomers for the formation of hybrid O–I products. They can be used, for example, as building blocks for the formation of highly ordered polyhedral oligomeric silsesquioxane (POSS) clusters<sup>14,15</sup> and as organosilane coupling agents for ceramic particle coatings.<sup>16,17</sup> [3-(Glycidyoxy)propyl]trimethoxysilane (GTMS) is one of the most popular trialkoxysilane-type precursors. The sol–gel polymerization of GTMS, used to form polysilsesquioxanes (SSQO) of the formula  $(RSiO_{3/2})_n$ , depends on the catalysis, solvent, amount of water used, and temperature. It is well known that under acid catalysis, loose, coil-like SSQO structures are formed, whereas basic catalysts promote fast polycondensation leading to compact, cagelike products.<sup>18</sup> These compact SSQO clusters are produced because of preferred intramolecular condensation, and the system finally becomes self-orga-

Correspondence to: M. Špírková (spirkova@imc.cas.cz).

Contract grant sponsor: Grant Agency of the Czech Republic; contract grant number: 203/01/0735.

Contract grant sponsor: Grant Agency of the Academy of Sciences of the Czech Republic; contract grant numbers: A4050008 and KSK4050111.

nized with (glycidyoxy)propyl groups issuing from the cluster. The size of the compact cages increases with increasing temperature and the dilution of the system.

The reactions and behavior of GTMS in the presence of colloidal silica particles have been studied by several authors.<sup>17,19–21</sup> The reaction mechanism is very complex, and the morphology and properties of the resulting coatings are considerably influenced by the method of their preparation. The best properties of these ceramic-particle-based coatings have been achieved when the acidic hydrolysis and alkaline polycondensation of GTMS in the presence of low-molecular-weight polyamine have been used.<sup>21</sup>

The topic of this article is the preparation and characterization of coating films (coatings) and free-standing films (films) made from two different functionalized organosilicon precursors and three different poly(oxypropylene)s end-capped with primary amino groups. The combination of several starting materials offers a rich variability of structures and final properties of the products. The combination of several analytical methods allows the study of the structure evolution from the pregel stage up to the structure and properties of the products. The mixed solvent (7:3 w/w water/alcohol) contributes to environmentally friendly reaction conditions. The influence of the organosilicon precursor functionality, the length and functionality of poly(oxypropylene) amines, the amino/epoxy molar ratio, and the presence/absence of colloidal silica particles on the product structure and properties have been studied and are discussed.

## EXPERIMENTAL

### Materials

GTMS (Fluka, Buchs, Switzerland), diethoxy[3-(glycidyoxy)propyl]methylsilane (GMDES; Fluka), Jeffamines D230, D400, and T403 (Huntsman Corp., Houston, TX), colloidal silica (40% solution in water,  $d_{\text{ave}} = 29$  nm; Ludox AS-40, Aldrich, Milwaukee, WI), propan-2-ol (IP, Lachema, Neratovice, Czech Republic), and 38% hydrochloric acid (Lachema) were used as received.

A detailed description of the starting materials is given in Table I.

### Preparation of the films and coatings

The films were prepared according to several recipes, which differed in the reaction time of alkaline polycondensation, the time and temperature of thermal curing, and so forth. The principal preparation steps were the following. First, the functionalized organosilicon precursors (GTMS and GMDES) were mixed with water, IP, and, in some cases, colloidal silica

particles, and the mixture was stirred at 400 rpm at the ambient temperature for 24 h. The pH was adjusted to 4 by the addition of dilute HCl. Under these conditions, the acidic hydrolysis step (used in the preparation of all the products) proceeded. Second, a solution of the oligomeric amine (50 wt % Jeffamine, 35 wt % water, and 15 wt % IP) was added, and the reaction mixture was stirred (400 rpm) at the ambient temperature for up to 2.5 h. Because of Jeffamine, the alkalinity of the resulting reaction mixture increased to pH 8–9, and alkaline polycondensation took place. Third, the reaction mixture was spread on glass or modified polypropylene sheets with a ruler to a constant thickness. The sheets were immediately placed in an oven and kept at 80 and 105°C (all products) and, in some cases, 130°C (see Table II for the details). At an elevated temperature, the thermal curing step finalized the preparation of all the films. All the preparation recipes (the details of which are given in Tables III–V) are summarized in Table II.

The following combinations of materials and ratios were used:

- [GTMS]/[GMDES] = 1:0 to 0:1 (w/w).
- [SiO<sub>2</sub>]/[GTMS + GMDES] = 0 or 1:3 (w/w).
- Molar ratio  $r = [\text{NH}]/[\text{epoxy}] = 0.8\text{--}2.5$ .
- Solvent (7:3 w/w water/IP) weight = 20–80 wt %.

### Methods of characterization

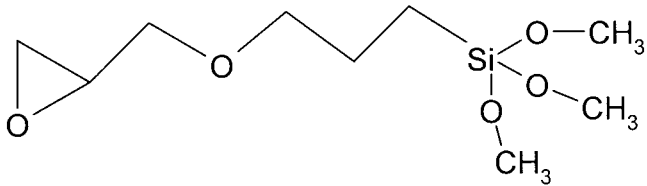

#### NMR spectroscopy

<sup>1</sup>H, <sup>13</sup>C, and <sup>29</sup>Si single-pulse magic-angle-spinning (MAS) NMR spectra were measured with a Bruker (Karlsruhe, Germany) DSX 200 NMR spectrometer at frequencies of 39.75, 50.23, and 200.14 MHz for <sup>29</sup>Si, <sup>13</sup>C, and <sup>1</sup>H, respectively. Direct-polarization and cross-polarization (CP) techniques were used to acquire <sup>13</sup>C and <sup>29</sup>Si MAS NMR spectra of solid samples (films) after preparation. The MAS frequency was 4 kHz, and the B<sub>1</sub> field intensity (<sup>1</sup>H and <sup>29</sup>Si) was 62.5 kHz. The number of scans for the accumulation of <sup>29</sup>Si CP–MAS NMR spectra was 3600, the repetition delay was 10 s, and the spin-lock pulse was 2–5 ms.

#### Dynamic mechanical thermal analysis

The dynamic mechanical properties of the films were studied with an ARES apparatus (Rheometric Scientific, Piscataway, NJ). The samples (17 mm × 7.5 mm × 0.1 mm or 30 mm × 10 mm × 0.1 mm) were measured by oscillatory shear deformation at a constant frequency of 1 Hz and at a rate of heating of 3°C/min to determine the temperature dependence of the storage shear modulus ( $G'$ ) and loss shear modulus ( $G''$ ) from –100 to +100°C.

TABLE I  
Description of Materials

Code (concentration of functional groups)	Formula
GTMS ( $c_{\text{epoxy}} = 4.23$ mequiv/g)	
GMDES ( $c_{\text{epoxy}} = 4.03$ mequiv/g)	
D230 ( $c_{\text{NH}} = 17.39$ mequiv/g)	$\text{H}_2\text{N}-\underset{\text{CH}_3}{\text{CH}}-\text{CH}_2-\left(\text{O}-\underset{\text{CH}_3}{\text{CH}_2}-\text{CH}\right)_x-\text{NH}_2$
	$x = 2 - 3$
D400 ( $c_{\text{NH}} = 9.26$ mequiv/g)	$\text{H}_2\text{N}-\underset{\text{CH}_3}{\text{CH}}-\text{CH}_2-\left(\text{O}-\underset{\text{CH}_3}{\text{CH}_2}-\text{CH}\right)_y-\text{NH}_2$
	$y = 5 - 6$
T403 ( $c_{\text{NH}} = 12.82$ mequiv/g)	$\begin{array}{c} \text{CH}_3 \\   \\ \text{CH}_2-\left(\text{O}-\underset{\text{CH}_3}{\text{CH}_2}-\text{CH}\right)_x-\text{NH}_2 \\   \\ \text{CH}_3\text{CH}_2\text{C}-\text{CH}_2-\left(\text{O}-\underset{\text{CH}_3}{\text{CH}_2}-\text{CH}\right)_y-\text{NH}_2 \\   \\ \text{CH}_2-\left(\text{O}-\underset{\text{CH}_3}{\text{CH}_2}-\text{CH}\right)_z-\text{NH}_2 \\   \\ \text{CH}_3 \end{array}$
	$(x + y + z) = 5 - 6$

#### Tensile characterization

The static mechanical properties were measured on an Instron 6025 instrument (Instron Limited, High Wycombe, UK). The specimens [25 mm × 6 mm × (0.08 ± 0.02) mm] were tested at the laboratory temperature at a test speed of  $3.33 \times 10^{-2}$  mm/s. All the reported values are averages of at least five specimens.

#### Small-angle X-ray scattering (SAXS)

SAXS measurements were performed with an upgraded Kratky camera with a 60- $\mu\text{m}$  entrance slit and a 42-cm flight path (A. Paar, Graz, Austria). Ni-filtered Cu K $\alpha$  radiation ( $\lambda = 0.154$  nm) was used, and it was monitored with a positron-sensitive detector<sup>22</sup> (Joint Institute for Nuclear Research, Dubna, Russia), the

**TABLE II**  
Procedures Used for the Preparation  
of Hybrid O–I Products

Procedure	Alkaline polycondensation (h) at 23°C	Thermal curing (h)		
		80°C	105°C	130°C
A	1	2	1	0
B	1	2	1	1
C <sup>a</sup>	2.5	2	1	0
D <sup>a</sup>	2.5	2	1	1

<sup>a</sup> Achievable only for D230- and D400-based products. For details, see the tensile and thermomechanical characterization.

spatial resolution of which was approximately 0.15 nm. The intensities were taken in the range of the scattering vector,  $q = (4\pi/\lambda)\sin \theta$ , from 0.06 to 20 nm<sup>-1</sup> (where  $2\theta$  is the scattering angle). The measured intensities were corrected for the sample thickness and transmission, the primary beam flux, and the sample–detector distance.

#### Atomic force microscopy (AFM)

All measurements were performed under ambient conditions with a commercial atomic force microscope (NanoScope Dimension IIIa, MultiMode Digital Instruments, Santa Barbara, CA). An Olympus OMCL TR-400 oxide-sharpened silicon nitride probe for the

contact mode (spring constant = 0.02 N/m) and an Olympus OTESPA tapping-mode etched silicon probe (spring constant = 42 N/m, resonant frequency ~ 270 kHz) for the tapping mode were used. In the contact mode, the normal force of the tip on the sample was reduced, and it did not exceed 10 nN.

## RESULTS AND DISCUSSION

### Polymer network buildup

During the preparation of hybrid O–I products, two types of polymer network buildup processes are anticipated. First, inorganic structures are formed by the sol–gel process. The reactive alkoxy groups of GTMS and GMDDES undergo hydrolytic and polycondensation reactions [eqs. (1) and (2)]. Although the polycondensation of GTMS results in SSQO branched and crosslinked structures, the GMDDES monomer forms linear polysiloxanes. By the cocondensation of these monomers, the crosslinking density of the inorganic phase can be tuned. In addition, if colloidal silica particles are present in the reaction mixture, the reaction of their Si–OH groups with OH groups of hydrolyzed GTMS and GMDDES is also possible. Second, the organic polymer network is formed by the reaction between epoxy groups of GTMS or GMDDES and amino groups of Jeffamine [eqs.

**TABLE III**  
Composition and Characteristics of D230-Based Hybrid O–I Networks

Sample code <sup>a</sup>	SiO <sub>2</sub> :GTMS:GMDDES:D230	[NH]:[epoxy]	T <sub>g</sub> (°C), region <sup>b</sup>	ε <sub>b</sub> (%)	σ <sub>b</sub> (MPa)	E (MPa)	w (kJ/m <sup>2</sup> )
1C	0:80.4:0:19.6	1.0	41, G	2	8.4	892	1.3
1D	0:80.4:0:19.6	1.0	42, G	2	10.6	1090	1.7
2A	0:67.2:0:32.8	2.0	5, R	6.6	2.8	60	1.8
3C	0:0:81.0:19.0	1.02	24, M	18.5	3.5	24	8.3
4A	21.2:63.5:0:15.3	1.0	41, G	2.1	15.3	1060	3.2
4C	21.2:63.4:0:15.4	1.0	43, G	1.8	12.4	1634	2.2
5A	19.8:58.7:0:21.5	1.5	M	4.7	13	271	8.3
5C	19.8:58.7:0:21.5	1.5	20, M	9.2	26.2	660	37.4
6A	18.3:54.5:0:27.2	2.0	R	5.5	5.4	147	3.2
6C	18.2:54.6:0:27.2	2.02	R	12.8	6	85	6.4
7A	17.1:51.7:0:31.2	2.5	R	8.1	3.1	54	2.8
8C	21.1:47.6:16.0:15.3	1.0	33, G	6.1	21.6	1470	23.8
9C	21.2:42.2:21.4:15.2	1.0	36, G	6.2	19.5	897	18.1
10A	21.3:32.0:32.0:14.7	1.0	23, M	4.8	7.8	624	4.7
10C	21.2:31.9:31.8:15.1	1.0	37, G	6.4	18.7	500	14.6
10D	21.2:31.9:31.8:15.1	1.0	M	5.2	15.4	537	11.2
11C	21.3:21.1:42.5:15.1	1.0	M	5.9	6.2	222	4.8
12A	19.7:39.3:19.6:21.4	1.52	16, M	10.8	11.6	162	16.7
13A	18.0:40.4:13.5:28.1	2.0	R	8.2	5.4	90	6.6
14A	18.5:36.9:18.3:26.3	2.0	10, R	8.5	7.5	79	6.1
15A	18.5:27.7:27.6:26.2	2.0	R	8.9	5.3	76	5.6
16A	18.5:18.7:36.5:26.3	2.0	R	10.1	4.7	54	5.6
17C	21.4:0:63.8:14.8	1.0	25, M	9.5	3.3	41	3.2
18A	18.6:0:55.4:26.0	2.0	R	11.6	4.1	42	4.2

<sup>a</sup> For the preparation procedure, see Table II.

<sup>b</sup> G = glassy state; M = main transition region; R = rubbery state.

TABLE IV  
Composition and Characteristics of D400-Based Hybrid O-I Networks

Sample code <sup>a</sup>	SiO <sub>2</sub> :GTMS:GMDDES:D400	[NH]:[epoxy]	T <sub>g</sub> (°C), region <sup>b</sup>	ε <sub>b</sub> (%)	σ <sub>b</sub> (MPa)	E (MPa)	w (kJ/m <sup>2</sup> )
19C	0:69.3:0:30.7	1.0	2, R	4.5	2.6	61	0.7
20C	0:52.2:0:47.8	2.0	-16, R	7.8	1.8	26	1.7
21C	0:0:69.5:30.5	1.02	R	8.4	2.1	14	0.9
22A	18.2:54.6:0:27.2	1.1	R	7.2	6.2	112	5.7
23A	15.5:45.5:0:39.0	2.02	R	9.4	4.3	57	4.5
24A	18.8:28.1:28.0:25.1	1.0	R	7.1	4.3	72	3.6
24C	18.7:28.0:28.0:25.3	1.0	0, R	15.3	6.5	59	9
25C	17.8:26.6:26.7:28.9	1.22	-2, R	8.2	3.2	55	2.6
26C	16.5:24.7:24.8:34.0	1.54	R	8.4	2.1	34	1.6
27C	18.9:0:56.5:24.6	1.0	R	8	2.4	26	1.2

<sup>a</sup> For the preparation procedure, see Table II.

<sup>b</sup> G = glassy state; M = main transition region; R = rubbery state.

(3) and (4)]. The structure of the organic epoxy-amine network is governed by the molecular weight of the Jeffamine ( $M_{\text{Jeff}}$ ) and the functionality of the Jeffamine ( $f_{\text{Jeff}}$ ); the crosslinking density increases with decreasing  $M_{\text{Jeff}}$  and increasing  $f_{\text{Jeff}}$ . Also, the system composition, given by the ratio of the functional groups ( $r$ ), is

important for the network structure. The most perfect network with the highest crosslinking density is formed at the stoichiometric composition,  $r = 1$ .

This overall process can be described by a simplified reaction scheme. For the inorganic network buildup (sol-gel process),

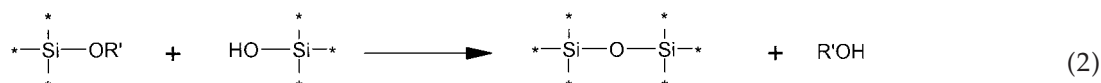
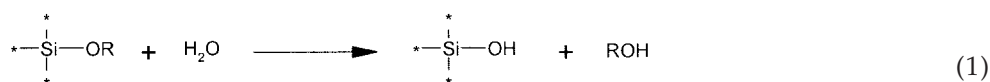


TABLE V  
Composition and Characteristics of T403-Based Hybrid O-I Networks

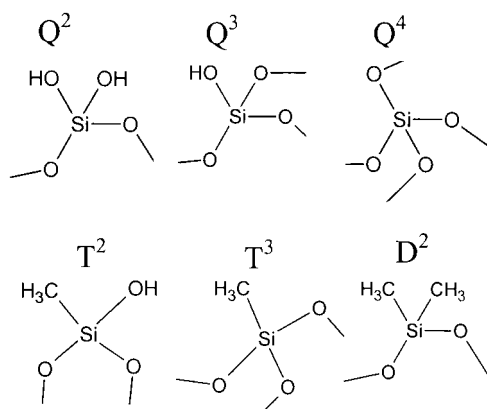
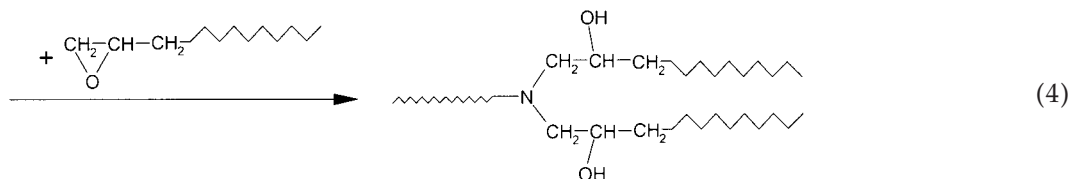
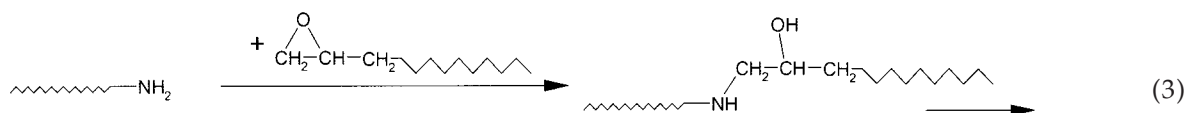
Sample code <sup>a</sup>	SiO <sub>2</sub> :GTMS:GMDDES:T403	[NH]:[epoxy]	T <sub>g</sub> (°C), region <sup>b</sup>	ε <sub>b</sub> (%)	σ <sub>b</sub> (MPa)	E (MPa)	w (kJ/m <sup>2</sup> )
28A	0:75.1:0:24.9	1.0	56; G	2.1	8.8	975	1.4
29A	0:0:75.5:24.5	1.0	17; M	31.2	7.3	31	30.5
30A	0:0:68.1:31.9	1.5	R	11.9	1.7	18	3.1
31B	20.6:62.0:0:17.4	0.84	54; G	1.6	11.9	1180	1.8
32A	20:60:0:20	1.0	41; G	2.3	12.1	1370	2.4
32B	20:60:0:20	1.0	G	1.5	8.5	1563	1.3
33A	18.5:55.4:0:26.1	1.5	36; G	3.7	25.8	1880	15.4
33B	18.5:55.4:0:26.1	1.5	G	1.8	39.5	3276	8.5
34B	20.1:40.1:20.2:19.6	1.0	40; G	3.9	4.5	207	2.4
35A	20.0:30.3:30.3:19.5	1.0	G	5	4.6	218	4.2
36A	21.3:0:65.6:15.1	0.78	R	7.4	2.6	44	2.2
37A	20.5:0:60.7:18.8	1.0	23; M	23.7	10.7	54	41.6
38A	18.5:0:55.4:26.1	1.5	R	9.3	2.1	27	2.8
39A	17.0:0:51.0:32.0	2.0	R	9.2	1.1	15	1.1

<sup>a</sup> For the preparation procedure, see Table II.

<sup>b</sup> G = glassy state; M = main transition region; R = rubbery state.

where R is an alkyl group, R' is a hydroxy or alkyl group, and \* is an (active) alkoxy group, hydroxy

group, or any other group inert in the process. For the organic network buildup,



**Scheme 1** Possible siloxane structural units of the prepared coating films.

The evolution of the inorganic structures is influenced not only by the type of organosilicon precursor but also by the presence or absence of colloidal  $\text{SiO}_2$  particles and by catalysis. It is well known that the shape, size, and properties of inorganic structures are strongly influenced by the mechanism of the sol-gel process (e.g., refs. 1–8, 16, and 21). This is why the kinetics and reaction mechanism of the polymerization reactions were studied by NMR spectroscopy first. The composition of the model reaction mixture was adjusted to enable the study of the individual reaction steps. The analysis of  $^1\text{H}$ ,  $^{29}\text{Si}$ , and  $^{13}\text{C}$  MAS NMR spectra of various reaction mixtures containing GTMS, GTMS, and silica under acid and alkaline conditions has revealed that during acidic hydrolysis, fast hydrolysis and the formation of short oligomers (dimers, trimers, and tetramers) are the predominant processes in the systems without colloidal silica. The formation of short oligomers is indicated by the presence of small amounts of  $\text{T}^2$  structure units (for details, see Scheme 1) detected in  $^{29}\text{Si}$  MAS NMR spectra (at ca.  $-58$  ppm) in the reaction mixture GTMS-pH 4 [see

Fig. 1(a)]. Although extensive polycondensation starts predominantly during the second alkaline polycondensation step, the rate of condensation reactions increases strongly in the presence of colloidal silica in the reaction mixture, even in the first acid-catalyzed process. This follows from the formation of a large number of  $\text{T}^3$  structure units ( $\sim 68$  ppm), as shown in Figure 1(b). It seems that  $\text{NH}_4^+$  ions, which stabilize colloidal silica particles, promote condensation reactions even at pH 4. Similar results were obtained for systems containing GMDES. Additionally,  $^1\text{H}$  and  $^{13}\text{C}$  MAS NMR spectra show that almost no cleavage of oxirane rings occurs during acidic hydrolysis and alkaline polycondensation before the thermal curing; this leaves oxirane groups available for the reactions, resulting in the formation of an organic network during the thermal curing step [see Fig. 2(a,b)].  $^{13}\text{C}$ -NMR signals of corresponding structure units (epoxide  $\text{OCH}_2$  ring at 44 ppm and epoxide  $\text{O-CH}$  at 51 ppm) gradually grow as a result of condensation reactions; however, their integral intensities remain constant. The signal broadening reflects gradual polycondensation in the nanocomposite product. The changes in the shape and position of the  $\text{CH}_2\text{Si}$  carbon signal ( $\sim 10$  ppm) also suppose hydrolysis and polycondensation. An increase in the signal intensity corresponding to methanol (ca. 49 ppm) and the disappearance of or a decrease in the  $\text{Si-OCH}_3$  signal (ca. 50 ppm) confirm a high rate of hydrolysis, which is almost complete within several hours, as shown in Figure 2(a,b). An almost 100% conversion of alkoxy groups of GTMS occurs within 6 h, whereas the cleavage of oxirane groups does not yet start in this reaction step.

Although the condensation reactions are almost complete before the last thermal curing step, their rate increases with the temperature in the final preparation step, even though the epoxy-amine polyaddition is the predominant reaction at elevated temperatures. The acceleration of condensation reactions may be deduced from  $^{29}\text{Si}$  MAS NMR spectra (not shown

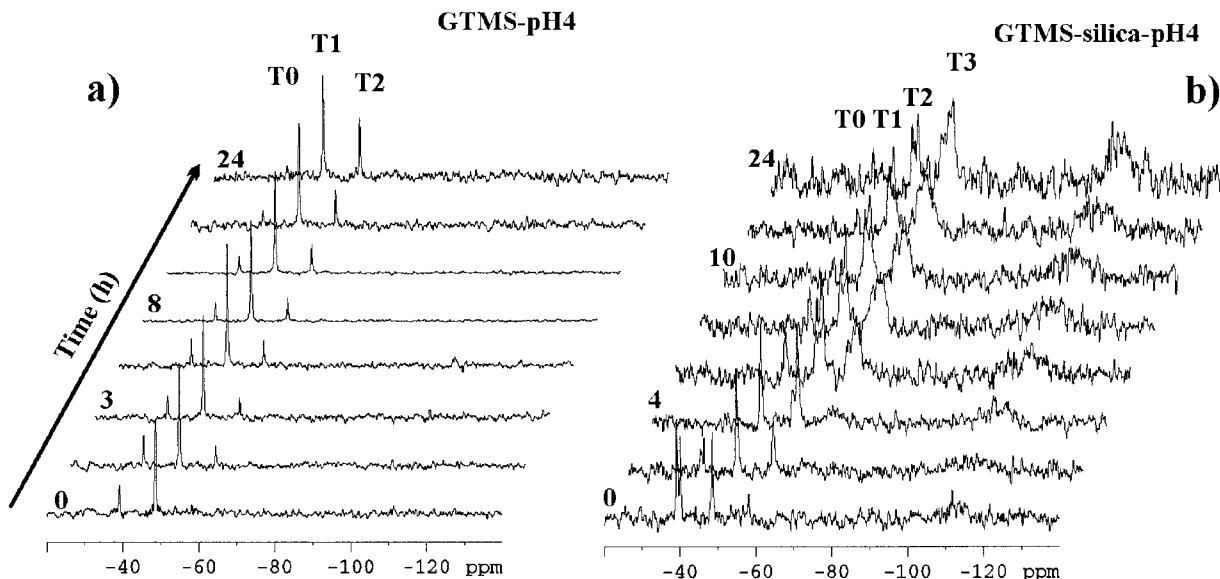


**Figure 1** <sup>29</sup>Si MAS NMR spectra of reaction mixtures (a) GTMS-pH4 and (b) GTMS-silica-pH4 measured at various reaction times.

here). The thermal treatment (A or C) of the GTMS-containing system at 80°C leads to a condensation degree of  $q = 0.94$ , whereas the subsequent treatment at 105°C results in a bit higher value of  $q = 0.96$ . The time-dependent NMR data also suggest the formation of more compact polycyclic structure units, as reflected by low-field shifts of <sup>29</sup>Si-NMR signals of the T<sup>3</sup> structure units.

The NMR analysis of a series of model reaction mixtures has confirmed that during the first reaction step, mainly hydrolysis but also partial condensation occur and that the presence or absence of colloidal SiO<sub>2</sub> influences substantially the extent of the conden-

sation reactions. In the second step, Jeffamine plays the role of a polycondensation catalyst in the sol-gel process only, whereas the epoxy groups remain almost untouched. Hence, during the alkaline polycondensation, a variety of inorganic clusters with pendant epoxy groups can be formed. In the final thermal curing step, the following processes proceed: (1) the completion of polycondensation reactions; (2) the massive buildup of the organic network by epoxy-amine polyaddition reactions, which start only with the heating of the reaction mixture [eqs. (3) and (4)];<sup>15</sup> and (3) the evaporation of water and alcohols (solvent and hydrolytic products).

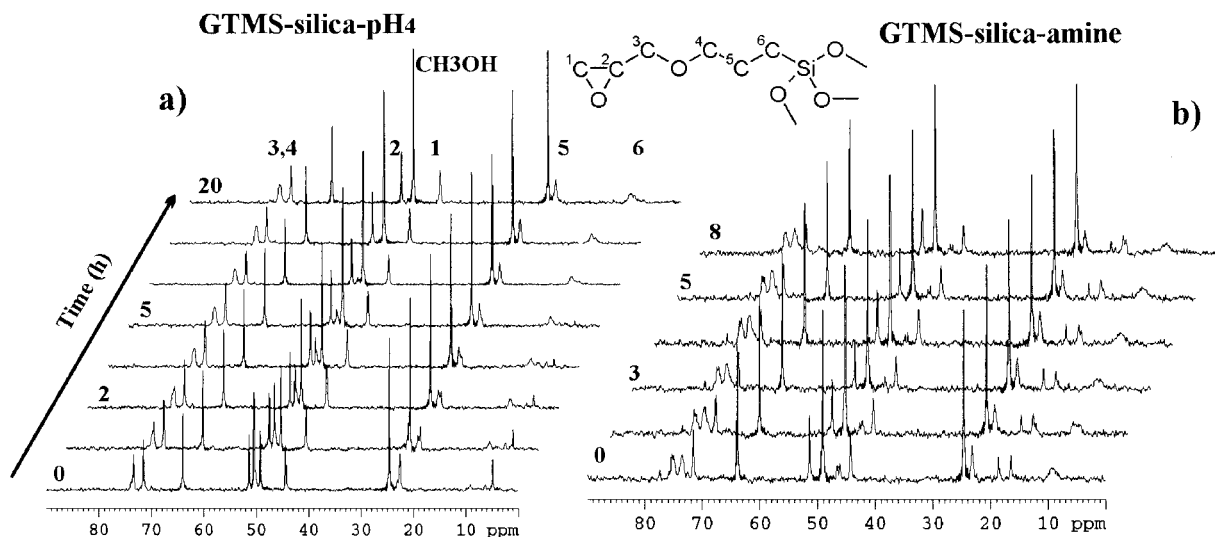


**Figure 2** <sup>13</sup>C MAS NMR spectra of reaction mixtures (a) GTMS-pH4 and (b) GTMS-silica-amine measured at various reaction times.

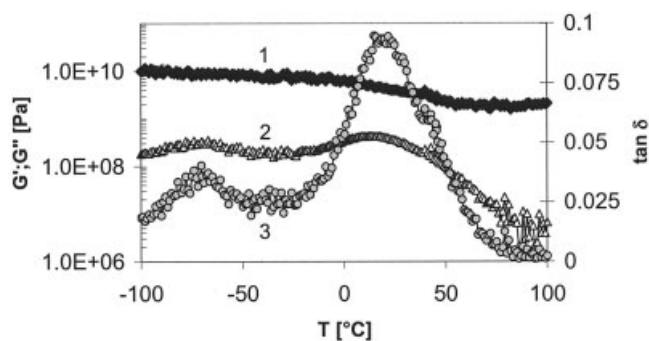


**Figure 3** (1)  $G'$ , (2)  $G''$ , and (3)  $\tan \delta$  as functions of temperature.

### Mechanical analysis

The ultimate goal of the study is the preparation of durable and mechanically resistant coatings and the determination of the conditions needed for their reproducible preparation. Most resistant coatings and films are made from reaction mixtures that are 40–60 wt % solvent. Therefore, all the products were prepared from mixtures that were 50 wt % solvent. The compositions of the initial reaction mixtures are given in Tables III–V, along with the specifications concerning the absence and presence of  $\text{SiO}_2$  nanoparticles, the GTMS, GTMS–GMDES, and GMDES products, the ratio of functional groups ( $r$ ), and the preparation procedure. Tables III–V deal with D230, D400, and T403 products, respectively.

The properties of polymer networks depend on the temperature, and a dramatic change occurs mainly in the region close to the glass-transition temperature ( $T_g$ ). Because the protecting coatings are subject to weather and temperature changes, it is necessary to study their temperature-dependent behavior in detail. Therefore, the dynamic mechanical properties [ $G'$ ,  $G''$ , and loss factor ( $\tan \delta$ )] of selected samples were measured from  $-100$  to  $100^\circ\text{C}$ .  $T_g$ 's were determined as the maxima of  $\tan \delta$  ( $\tan \delta = G''/G'$ ) versus the temperature ( $T$ ). The  $G'$  values of all the analyzed samples were within the range of  $10^3$ – $10^4$  MPa in the glassy state for  $T = T_g - 75^\circ\text{C}$  and within the range of  $10^2$ – $10^3$  MPa in the rubbery state for  $T = T_g + 50^\circ\text{C}$ . The high values of  $G'$  for the films at temperatures above  $T_g$  are the result of a high crosslinking density of the organic network, but they are mainly due to the reinforcing effect of the inorganic structures formed *in situ* by admixed silica and silsesquioxane clusters. Figure 3 shows a typical temperature dependence of  $G'$ ,  $G''$ , and  $\tan \delta$ . All the prepared films show a two-phase morphology with two relaxation peaks of  $\tan \delta$  dependences. The low-temperature maximum at  $T = -70 \pm 3^\circ\text{C}$  corresponds to the relaxation of the polyoxypropylene chain of the Jeffamine used. The more distinct maximum between  $-16$  and  $+56^\circ\text{C}$  can

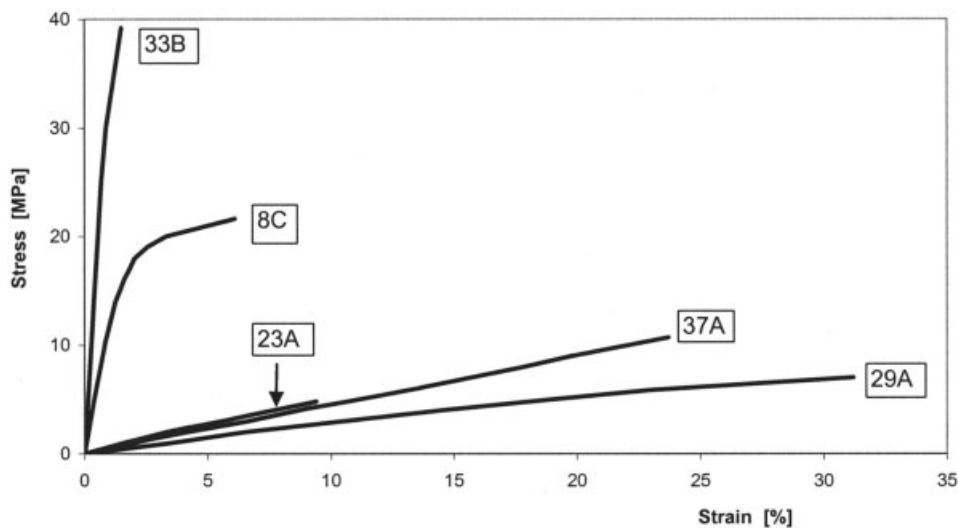
be attributed to the glass transition of the organic phase immobilized by *in situ* formed inorganic structures and by admixed silica. The O–I interface interaction is quite strong, and there is a reduction in the originally large fraction of organic chains, as we can see from a comparison of the amplitudes of  $G''(T)$  peaks in Figure 3 corresponding to both free and immobilized chains. As a result, the glass transition of this interphase mainly governs the thermomechanical behavior of the films. Therefore, from an application point of view, we are interested mainly in this high-temperature relaxation manifested in  $T_g$  of the film. The values of  $T_g$ , together with the state in which the product exists at  $23^\circ\text{C}$ , are listed in Tables III–V.

One of the potential applications of the prepared products is their use as protecting coatings on glass-like surfaces. Information on their tensile properties at room temperature is, therefore, needed. The products with the most promising properties at ambient temperatures are discussed in detail. All the stress–strain characteristics discussed were measured at  $23^\circ\text{C}$ , and the strain at break ( $\epsilon_b$ ), stress at break ( $\sigma_b$ ), toughness ( $w$ ; i.e., the energy per unit of the cross section necessary to break the sample), and Young's modulus ( $E$ ) of the films were determined. The tensile properties were proved not to be influenced by the film thickness in the region of 0.06–0.1 mm. Therefore, we carried out all measurements within this thickness region to obtain comparable results for all the samples. The tensile properties are summarized in Tables III–V. It is evident that the products differ substantially in their tensile properties [Fig. 4(a)] as a result of the variation of the product structure (organic and inorganic). We have divided our systems into three categories according to their state at the ambient temperature; this is crucial for possible material applications as protective coatings.

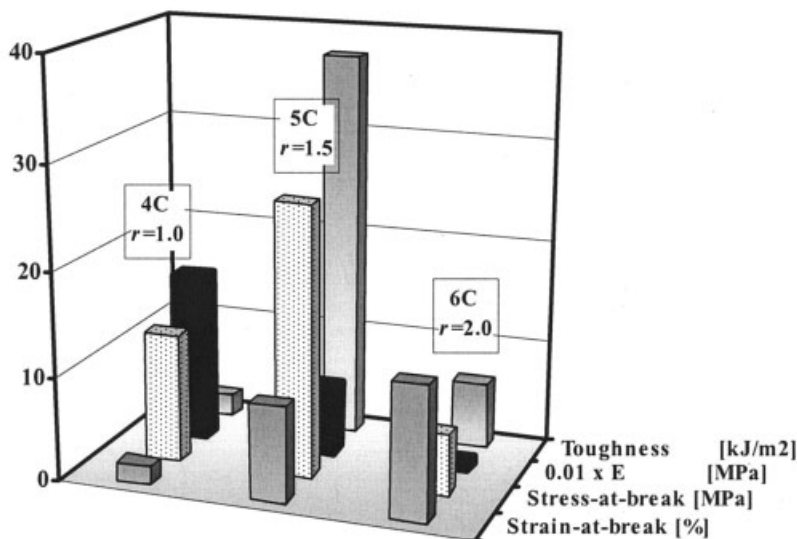
### Glassy-state region

The films with  $T_g > 30^\circ\text{C}$  are characterized by high values of  $E$  at the ambient temperature ( $E > \text{ca. } 800$  MPa), relatively high values of  $\sigma_b$  (mostly  $>10$  MPa), and low values of both  $\epsilon_b$  (mostly  $<2\%$ ) and  $w$  (largely  $<3$  kJ/m<sup>2</sup>). The systems showing a high crosslinking density of both organic and inorganic networks belong to this category. It includes the hybrids based on D230 and T403 Jeffamines with stoichiometric compositions or a slight off-stoichiometry of the organic network and only a small fraction of bifunctional GMDES present in the inorganic phase. The addition of the silica particles to the hybrid leads to an increase in  $E$ ,  $\sigma_b$ , and  $w$  of the glassy products (cf. samples 1C vs 4C and 28A vs 32A in Tables III–V). However, the variation of the curing regimes has no significant effect, resulting only in a slight increase in the glassy modulus when a longer polycondensation step (C or D





(a)



(b)

**Figure 4** (a) Stress–strain dependence of selected free-standing films. The compositions of the samples were as follows: 8C, SiO<sub>2</sub> + 3:1 GTMS/GMDES + D230 ( $r = 1.0$ ); 23A, SiO<sub>2</sub> + GTMS + D400 ( $r = 1.0$ ); 29A, GMDES + T403 ( $r = 1.0$ ); 33B, SiO<sub>2</sub> + GTMS + T403 ( $r = 1.5$ ); and 37A, SiO<sub>2</sub> + GMDES + T403 ( $r = 1.0$ ). The temperature was 23°C. (b) Effect of molar ratio  $r$  (NH groups/epoxy groups) on the tensile properties of the films made from SiO<sub>2</sub>, GTMS, and D230. The temperature was 23°C.

procedure) or high-temperature curing (B or D) is applied (cf. samples 4A vs 4C, 1C vs 1D, 32 A vs 32 B, and 33A vs 33B). For details, see Table II–V.

Main transition region

The films showing lower  $T_g$ 's and existing in the main transition region at the ambient temperature ( $T_g \sim$

20°C) have relatively high values of  $w$  (mostly >10 kJ/m<sup>2</sup>) as a result of high values of  $\sigma_b$  (mostly >15 MPa) and medium values of  $\epsilon_b$  (>5%). The hybrids belonging to this group show a lower crosslinking density of the organic network due to an off-stoichiometric composition,  $r > 1.5$  (excess of amine), or a high fraction of GMDES reducing the crosslinking density of the inorganic network. Typical representatives of

this group are T403-based networks with the inorganic phase formed by GMDES only (samples 29A and 37A) and off-stoichiometric D230-based systems,  $r = 1.5$ , with GTMS or those with an excess of GMDES in the inorganic phase (samples 5C, 10A, 12 A, 3C, and 17C). An outstanding value of  $w$  at the ambient temperature was achieved in the hybrids of this category (e.g., samples 29A and 37A) because of their lower crosslinking density and the presence of long, linear polysiloxane chains. Moreover, procedure C, promoting polycondensation, seems to improve the properties of D230-based products in comparison with procedure A.

#### Rubbery-state region

The rubbery films with  $T_g < 15^\circ\text{C}$  have relatively high values of  $\varepsilon_b$  (mostly  $>8\%$ ), acceptable values of  $\sigma_b$  (mostly  $>4$  MPa), and relatively low values of  $E$  ( $\leq 10^2$  MPa). The values of  $w$  (largely  $>4$  kJ/m<sup>2</sup>) are higher than those of glassy samples but lower than those of samples belonging to the main-transition-region category. Rubbery behavior at the ambient temperature was observed in the hybrid systems of the lowest crosslinking density of the epoxy-amine network, that is, in D230-based (e.g., samples 2A, 6C, and 7A) and T403-based (e.g., samples 29A, 30A, and 36A) systems with a high amine excess,  $r \geq 2$ , and in all D400-based networks. In addition, the hybrids containing in their inorganic structures only linear polysiloxane chains from GMDES are in the rubbery state. The addition of colloidal silica particles results in an increase in  $E$  and improves  $\sigma_b$  while keeping unchanged  $\varepsilon_b$ . Consequently,  $w$  is generally higher for silica-containing products than for silica-free analogues. Procedure C surprisingly leads to products with lower values of  $E$ , higher values of  $\varepsilon_b$ , and higher values of  $w$  in comparison with procedure A (cf. samples 6A vs 6C and 24A vs 24 C).

#### Tensile and thermomechanical characterization

With respect to the applications of hybrid films to protective coatings, we studied the influence of the composition of the reaction mixture and the conditions of preparation on the thermomechanical properties. We tested the effects of the presence of SiO<sub>2</sub> particles, the GTMS/GMDES ratio, and the NH/epoxy ratio.

#### SiO<sub>2</sub> presence/absence

Silica particles in a system generally serve as reinforcing fillers. We have found that the addition of SiO<sub>2</sub> nanoparticles into the reaction system has only a negligible effect on  $T_g$  (cf. samples 1C vs 4C, 3C vs 17C, 28A vs 32A, and 29A vs 37A). The presence of silica,

however, reduces  $\varepsilon_b$ , mainly in samples in the transition region, and increases  $\sigma_b$ ,  $E$ , and  $w$  in most cases (cf. samples 1C vs 4C, 2A vs 6A, 3C vs 17C, 28A vs 32A, 29A vs 37A, and 30A vs 38A). This finding is very important from a practical point of view, that is, for scratch-resistant protection applications.

#### GTMS/GMDES ratio

Changing the ratio, we can effectively tune the structure of the *in situ* formed inorganic clusters. When GTMS was replaced by GMDES, other conditions being kept constant, more flexible products with linear polysiloxane chains were obtained with substantially lower  $T_g$ 's. This effect was observed for both SiO<sub>2</sub>-containing and SiO<sub>2</sub>-free films (cf. samples 1C vs 3C, 28A vs 29A, and 32A vs 37A). In some cases, the increase in the GMDES fraction caused the transition from the glassy-region state to the main-transition-region state of the film at the ambient temperature (see T403-based products or samples 4C and 17C for D230-based films). This finding allows for the tuning of the mechanical properties of the products through the adjustment of the GTMS/GMDES ratio.

#### Type of jeffamine

The choice of the Jeffamine determines the structure of the organic network and influences strongly the properties of prepared films. All D400-based films had low  $T_g$ 's and were rubbery at 23°C. The D230- and T403-based products showed a higher crosslinking density of the organic network and made it possible to prepare films with a broader span of mechanical properties; for details, see Tables III and V.

#### Composition of the organic phase

The [NH]/[epoxy] ratio, or  $r$ , is another way of controlling the organic network density affecting  $T_g$  of a system. The shift from the stoichiometric composition ( $r = 1.0$ ) to the systems with an amine excess ( $r > 1$ ) results in a significant decrease in  $T_g$  (cf. samples 1C vs 2A and 19C vs 20C). This means that by changing the composition of the organic phase, we can achieve the transition of the products from one state to another (from the glassy state to the main transition region and to the rubbery state; cf. samples 4A, 5A, 6A, and 7A or samples 4C, 5C, and 6C). The tensile properties of some typical representatives are shown in Figure 4(b). The hardest material with the highest modulus was prepared with the stoichiometric composition. However, high  $w$  and  $\sigma_b$  values were achieved in the films in the main transition region at ambient temperatures, requiring synthesis from an off-stoichiometric mixture:  $r = 1.5$  for SiO<sub>2</sub>-GTMS-D230 products ( $T_g$

= 20°C) and  $r = 1.0$  for SiO<sub>2</sub>-GMDES-T403 samples ( $T_g = 23^\circ\text{C}$ ).

### Preparation technique

Four types of preparation techniques, differing in the curing regimes, were tested. The hydrolytic step was kept the same in all cases; however, the sol-gel polycondensation stage and the final thermal curing varied. Tables III–V contain the specifications of the methods of preparation (the first column in Table II). For the T403 systems, only variants A and B could be used to prevent gelation during the polycondensation step. It was found that (besides the influence of the type of reactant used, as discussed previously) the curing regime could change the tensile properties. The most important step influencing these properties is the alkaline polycondensation stage because the inorganic clusters formed during this step affect substantially the final morphology on the submicrometer scale. However, we have not found any universal technique of preparation to obtain products with optimum properties. The data suggest that the final hybrid O–I network is formed by a complex mechanism, which results in a broad variation of mechanical properties (for details, see Tables III–V).

### Structure and surface characterization

The structure of the products—films and coatings—was studied with SAXS and NMR spectroscopy. The surface morphology was investigated with AFM.

In Figure 5(a–c), SAXS data of hybrid O–I networks are shown. The sharp interference maxima in the SAXS profiles prove that an ordered O–I two-phase structure is formed in the networks obtained by the polymerization of GTMS with amines [D230, D400, and T403; Fig. 5(a)]. The interference maxima in the region of  $q = 2.3\text{--}3.3\text{ nm}^{-1}$  correspond to correlation distances of 1.9–2.7 nm. The correlation distance depends on the chain size of the amine spacer and on the amine/epoxy ratio,  $r$ . The second broad maximum, observed at  $q$  values higher than  $5\text{ nm}^{-1}$  on all SAXS curves of samples obtained by GTMS polymerization, can be attributed to the inner structure. However, no regular arrangement has been observed in networks obtained through the polymerization of GMDES [Fig. 5(b)]. This fact can be explained by the different functionalities of GTMS and GMDES for the buildup of inorganic domains. Although trifunctional GTMS can form highly ordered and cagelike POSS clusters,<sup>18</sup> difunctional GMDES can only slightly lengthen the chains of inorganic clusters. The structural arrangement of our GTMS-containing products indirectly proves the form of the compact structures formed. According to SAXS experiments, the presence of silica particles does not disturb the structure ordering of

hybrid O–I films [Fig. 5(c)]. However, NMR data indicate that colloidal SiO<sub>2</sub> interacts with O–I networks and may form a low fraction of chemical bonds within the network (see later). The structure of the product films (samples 5C and 37A) was evaluated through an analysis of the <sup>13</sup>C and <sup>29</sup>Si CP–MAS NMR spectra, which are shown in Figure 6(a–d). From a comparison of the <sup>13</sup>C CP–MAS NMR spectra of both systems [cf. Fig. 6(a,b)], we find that the system based on GTMS (5C) is more regularly organized than that based on GMDES, as proved by a large inhomogeneous broadening of the signals in the aliphatic region for sample 37A. Although it is generally recognized that the reactivity of alkoxy(alkyl)silanes increases with an increasing number of alkyl substituents, it has to be stressed that the extent of condensation reactions of GTMS ( $p = 0.96$ ) is much higher than that of GMDES [ $p = 0.73$ ; see Fig. 6(c,d)]. A fairly high amount of T<sup>3</sup> structure units observed by NMR indicates the formation of highly condensed and compact cagelike clusters, which are surrounded by the organic phase. The resulting material can be considered nanoheterogeneous with partly separated organic and silicon-containing phases. However, the presence of a large amount of D<sup>1</sup> structure units confirms that nearly 54% of the GMDES monomer units are terminal chain units and provide only linkage with the organic phase. This results in the softening of the final coatings (larger elasticity). Furthermore, the condensation of surface hydroxy groups from colloidal silica particles and GTMS or GMDES silanol groups has also been observed. It is indicated by the decreasing NMR intensity of Q<sup>3</sup> and Q<sup>2</sup> structure units in colloidal silica particles of composite systems with the reaction time. Although this decrease is small (ca. 1–2%), the NMR analysis supports covalent bonding between the inorganic and organic phases.

The surface morphology was investigated with AFM. AFM measurements in the tapping and contact modes were compared to test whether the destruction of the surface occurred and influenced the results in the contact mode. In both cases (i.e., in the tapping mode and contact mode with the least tip force on the sample surface possible), practically identical images were obtained, and so identical information was obtained on the surface morphology for all the prepared O–I hybrid coatings (even for samples with low surface hardness). The coatings have fairly flat and regular surfaces, their smoothness and profile depending on the presence or absence of colloidal SiO<sub>2</sub> particles. On the nanometer scale, the presence of individual SiO<sub>2</sub> particles at the surface is quite apparent (Fig. 7). They are distributed quite uniformly, without distinct clustering, and they are well incorporated into the surface layer. On the basis of the stoichiometry and average distances between the silica particles in the surface layer, it has been found that SiO<sub>2</sub> nanopar-

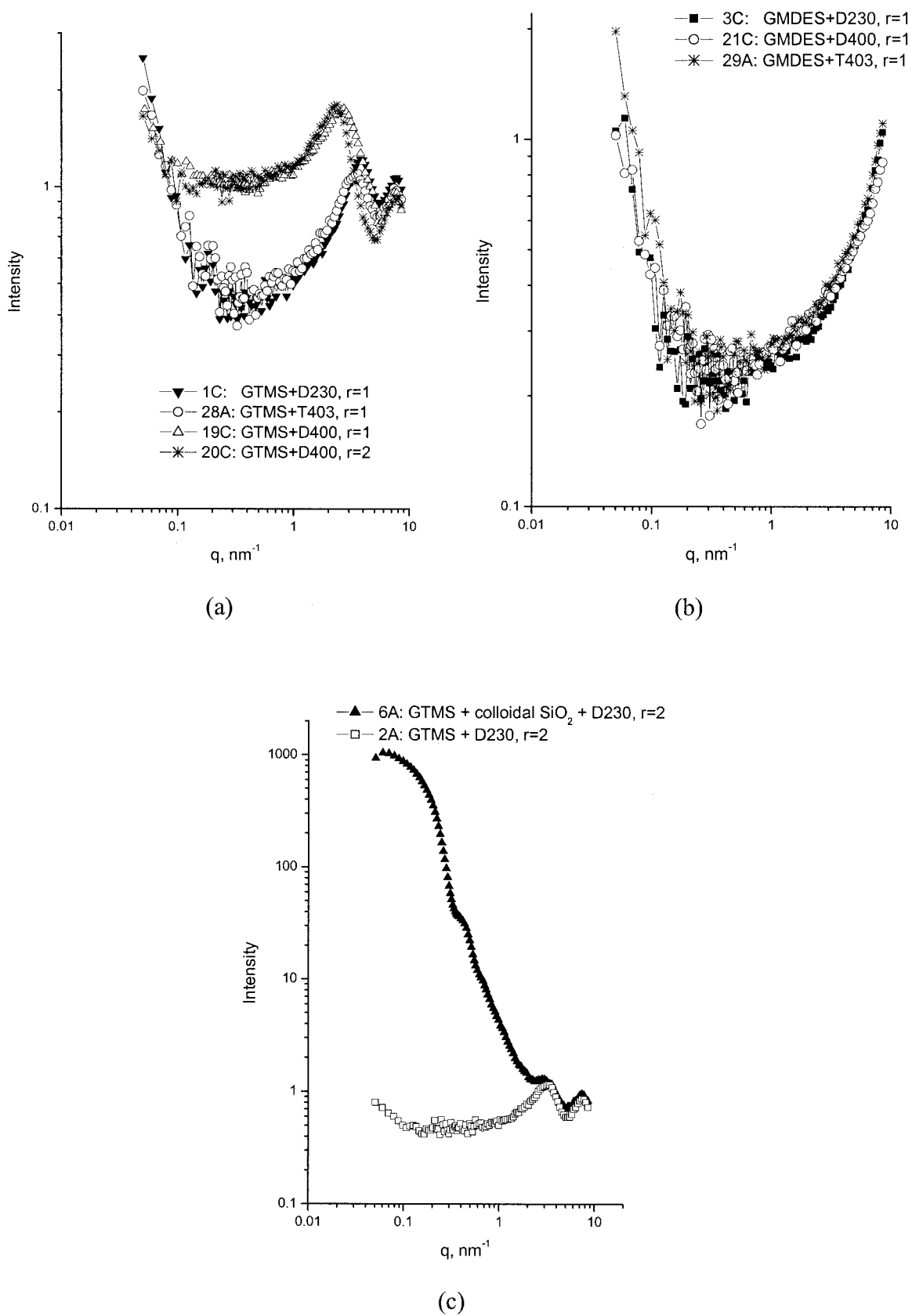


**Figure 5** SAXS curves of the O-I networks: (a) GTMS-based films, (b) GMDES-based films, and (c) SiO<sub>2</sub>-containing and SiO<sub>2</sub>-free analogues.

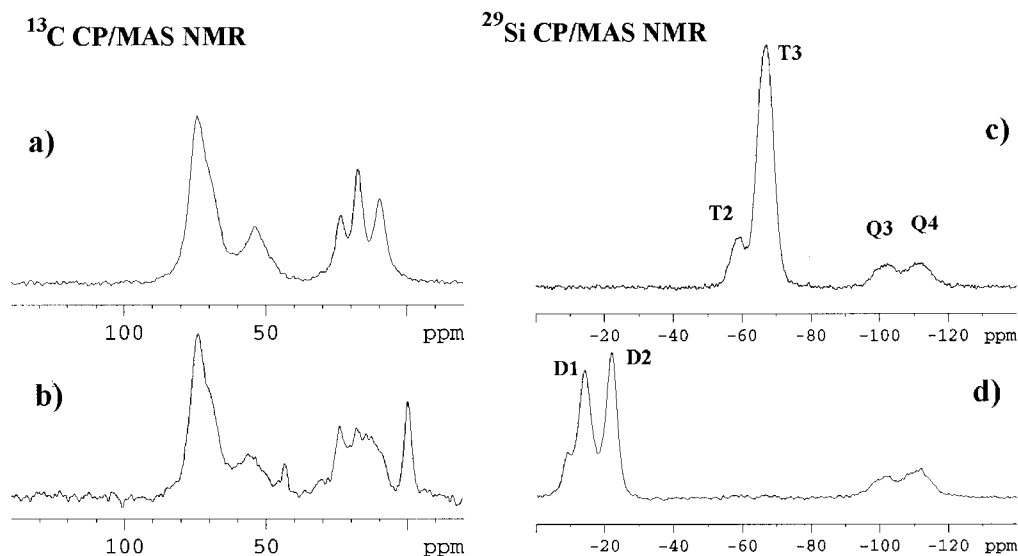


Figure 6  $^{13}\text{C}$  and  $^{29}\text{Si}$  CP-MAS NMR spectra of (a,c) sample 5C and (b,d) sample 37A.

ticles, which are quite miscible with all the reactants and are fairly compatible with the formed O-I networks, concentrate in the surface layer, thus lowering the surface tension (for details, see ref. 23). They remain uniformly distributed in the three-dimensional structure, and a significant fraction of these particles still remain in the bulk of the O-I hybrid film, as indicated by the random distribution of  $\text{SiO}_2$  particles revealed by SAXS.

### CONCLUSIONS

Hybrid O-I coatings and free-standing films have been prepared and characterized. On the basis of NMR spectroscopy, we have proposed and discussed a possible reaction mechanism of the organic and in-

organic network buildup process. It has been confirmed that in particular steps of the preparation, different reactions predominate: hydrolysis in the first step, polycondensation in the second, and mainly epoxy-amine polyaddition in the final step. The presence of colloidal  $\text{SiO}_2$  significantly promotes condensation reactions in the acid-catalyzed step.

The difference in the tensile properties has been discussed from two points of view: (1) the state of matter of products at the ambient temperature ( $23^\circ\text{C}$ ) and (2) the influence of individual reactants, the system composition, the reaction conditions, and the techniques of preparation on the tensile properties. Products have been prepared, ranging from the glassy region to the main transition region to the rubbery state at room temperature. Hard protective films have been obtained mainly from systems based on T403 Jeffamine and GTMS in the presence of silica particles. Even hybrids with a slight amine excess show high moduli and tensile strengths ( $\sigma_b$ ). If  $w$  is taken as the criterion for the optimization of the reaction conditions and procedure, only a limited number of products can be selected; nevertheless, their properties may be tuned through changes in the reaction composition and conditions. O-I films with suitable  $w$  values have  $T_g$ 's close to  $20^\circ\text{C}$ , although the composition, preparation technique, and tensile properties vary. Typical representatives of these products with above-average values of  $w$  are GTMS-D230 at the  $[\text{NH}]/[\text{epoxy}]$  ratio ( $r$ ) of approximately 1.5 and stoichiometric GMDES-T403 systems.

$T_g$  of the films is easily tuned by the modification of the buildup of the organic network and inorganic structures, and this makes it possible to affect the tensile properties. Several methods of controlling  $T_g$

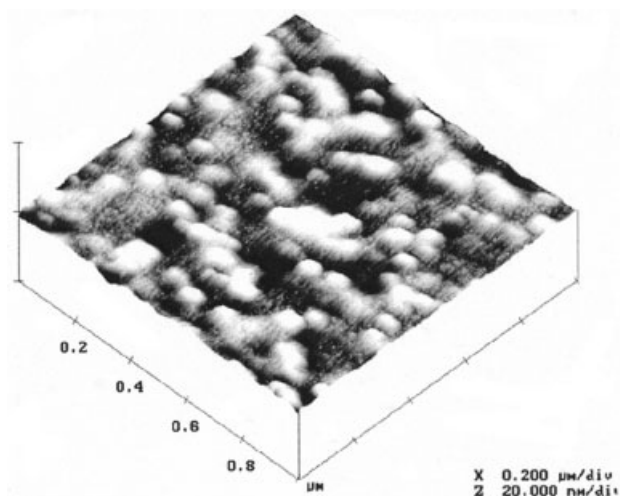


Figure 7 Three-dimensional image of the surface of sample 37A ( $\text{SiO}_2 + \text{GMDES} + \text{T403}$ ;  $r = 1.0$ ) in the contact mode.

have been tested; it has been reduced (1) by changes in the composition as  $r$  increases, (b) by the replacement of T403 or D230 Jeffamines with longer D400, and (c) by the replacement of GTMS with bifunctional GMDES.

The structural characterization of the final products, performed with SAXS and NMR, has confirmed that GTMS-based products differ substantially from their GMDES-based analogues. Although GTMS-based products exhibit a certain kind of ordering, GMDES-based products do not show any regular arrangement. NMR experiments have also confirmed a higher condensation rate in GTMS-based systems than in GMDES-based systems. All the products have flat and regular surfaces. If colloidal silica particles are present in the reaction mixture, they are well incorporated into the surface layer and may be detected by AFM.

The conditions for the reproducible preparation of suitable polymeric products have been found and optimized. They enable the tuning of their properties according to the intended use. Supplementary and more detailed studies on several selected products, aimed at the potential long-term use of the prepared films as scratch- and abrasion-resistant systems, are in progress and will be reported later.

## References and Notes

1. Brinker, C. J.; Scherer, C. W. *Sol-Gel Science*; Academic: San Diego, 1990.
2. Pouxviel, J. C.; Boilot, J. P.; Nelodil, J. C.; Lallemand, J. Y. *J Non-Cryst Solids* 1987, 89, 345.
3. Chang, S. Y.; Ring, T. A. *J Non-Cryst Solids* 1992, 147, 56.
4. Pope, E. J. A.; Mackenzie, J. D. *J Non-Cryst Solids* 1986, 87, 185.
5. Boonstra, A. H.; Bernards, T. N. M. *J Non-Cryst Solids* 1988, 105, 207.
6. Stevens, N. S. M.; Rezac, M. E. *Polymer* 1999, 40, 4289.
7. Fidalgo, A.; Nunes, T. G.; Ilharco, L. M. *J Sol-Gel Sci Technol* 2000, 19, 403.
8. Loy, D. A.; Baugher, B. M.; Baugher, C. R.; Schneider, D. A.; Rahimian, K. *Chem Mater* 2000, 12, 3624.
9. Wen, J.; Vasudevan, V. J.; Wilkes, G. L. *J Sol-Gel Sci Technol* 1995, 5, 115.
10. Metroke, T. L.; Knobbe, E. T. *Mater Res Proc Res Soc* 2000, 628, CC11.4.
11. Kasemann, R.; Schmidt, H. *New J Chem* 1994, 18, 1117.
12. Ni, H.; Johnson, A. H.; Soucek, M. D.; Grant, J. T.; Vreugdenhil, A. J. *Macromol Mater Eng* 2002, 287, 470.
13. Bauer, F.; Sauerland, V.; Gläsel, H.-J.; Ernst, H.; Findeisen, M.; Hartmann, E.; Langguth, H.; Marquardt, B.; Mehnert, R. *Macromol Mater Eng* 2002, 287, 546.
14. Lichtenhan, J. D.; Vu, H. Q.; Carter, J. A.; Gilman, J. W.; Ferer, F. J. *Macromolecules* 1993, 26, 2141.
15. Matějka, L.; Dukh, O.; Brus, J.; Simonsick, W. J.; Meissner, B. *J Non-Cryst Solids* 2000, 270, 34.
16. Daniels, M. W.; Francis, L. F. *J Colloid Interface Sci* 1998, 205, 191.
17. Daniels, M. W.; Francis, L. F. *Mater Res Proc Res Soc* 1999, 576, 313.
18. Matějka, L.; Dukh, O.; Hlavatá, D.; Meissner, B.; Brus, J. *Macromolecules* 2001, 34, 6904.
19. Daniels, M. W.; Chu, L.; Francis, L. F. *Mater Res Soc Symp Proc* 1996, 435, 215.
20. Daniels, W.; Sefcik, J.; Francis, L. F.; Cormick, A. V. M. *J Colloid Interface Sci* 1999, 219, 351.
21. Chu, L.; Daniels, M. W.; Francis, L. F. *Mater Res Soc Symp Proc* 1996, 435, 221.
22. Chernenko, S. P.; Cheremukhina, G. A.; Fateev, O. V.; Smykov, L. P.; Vasiliev, S. E.; Zanevsky, Y. V.; Kheiker, D. M.; Popov, A. N. *Nucl Instrum Meth Phys Res Sect A* 1994, 348, 261.
23. Špírková, M.; Brus, J.; Hlavatá, D.; Kamišová, H.; Matějka, L.; Strachota, A. *Surf Coat Int, Coat Trans B3* 2003, 86, 187.